

## Edge-state transport in finite antidot lattices

R. Schuster,\* K. Ensslin,<sup>†</sup> V. Dolgoplov,<sup>‡</sup> and J. P. Kotthaus

*Sektion Physik, Ludwig-Maximilians-Universität München, Geschwister-Scholl-Platz 1, D-80539 München, Germany*

G. Böhm and W. Klein

*Walter Schottky Institut, Technische Universität München, D-85748 Garching, Germany*

(Received 22 February 1995)

We study electron transport in an antidot superlattice with a finite number of periods. At low carrier densities and high magnetic fields the electrons travel phase coherently over the entire system in magnetic edge channels and interfere with each other under the influence of the geometry of the antidot potential landscape. The magnetoresistance displays pronounced Aharonov-Bohm-type oscillations arising from electrons that travel along the bound states that form around the antidots. The characteristic period of the oscillations is given by the area defined by the circumference of the antidots.

Antidot superlattices represent a model system to study electron transport through a periodic potential landscape.<sup>1-4</sup> Starting from a high-mobility two-dimensional electron gas (2DEG), a periodic array of potential pillars can be fabricated by various technological means. A typical potential landscape is sketched in Fig. 1(a), where the maxima of the potential peak through the

Fermi energy. So far most experiments have been performed on systems whose extensions are much larger than the electron mean free path  $l_e$  as well as the phase coherence length  $L_\phi$ . Pronounced maxima have been observed in the magnetoresistance arising from ballistic electron orbits around groups of antidots. The experimental observations have successfully been described by classical dynamics neglecting the phase of the electrons.<sup>5</sup>

Effects related to the phase coherence of the electrons along the classical trajectories have only recently been observed. Weiss *et al.* reported so-called quantum oscillations<sup>6</sup> that rely on the phase coherence on the length scale of the lattice period. Schuster *et al.* investigated a finite antidot lattice whose total dimension is smaller than  $L_\phi$  at low temperatures.<sup>7</sup> In this case the classical commensurability oscillations are superimposed by strong reproducible fluctuations in the magnetoresistance that die out at higher magnetic fields where the cyclotron diameter becomes smaller than the lattice period. The Fourier analysis reveals an Aharonov-Bohm (AB)-type effect related to the area enclosed by the respective classical cyclotron orbit around groups of antidots.

Usually the Fermi energy  $E_F$  in the antidot lattices investigated so far is relatively high [Fig. 1(a)] in the sense that the filling factor of the Landau levels that arise at finite magnetic field is typically larger than 10 for the magnetic fields of interest. Here we focus on a very different regime of low carrier densities and magnetic fields around a filling factor  $\nu=2$ . The system now schematically resembles a shallow lake (Fermi sea) between the antidot pillars [Fig. 1(b)]. The low Fermi level and the reduced screening of the electrons lead to relatively large antidots [see the transition from Fig. 1(a) to Fig. 1(b)]. Transport now occurs predominantly in edge states that also extend into the bulk of the sample because of the presence of the antidot lattice. The role of the classical electron trajectories as described previously is now taken over by quantum-mechanical edge states.

In order to investigate phase coherence effects in antidot systems we fabricate an array of  $9 \times 9$  antidots sur-

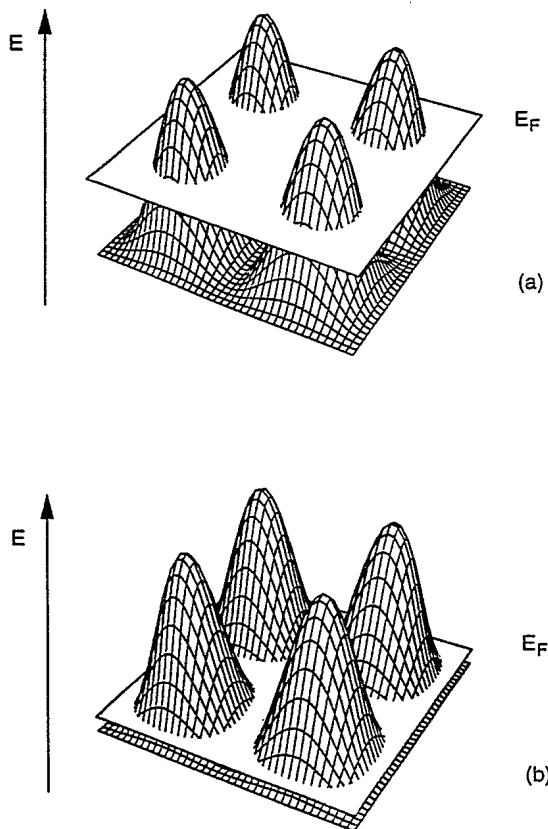


FIG. 1. Antidot potential with (a) a high Fermi energy and (b) a very low Fermi energy. The position of the Fermi energy is depicted by the white planes.

rounded by a square geometry (see the inset of Fig. 2). For very low temperatures where electron-electron scattering is reduced, both  $L_\phi$  and  $l_e$  may exceed the size of the system.<sup>8</sup> The electrons now carry a phase and an amplitude and therefore can interfere with each other.

The fabrication process starts from a GaAs/Al<sub>x</sub>Ga<sub>1-x</sub>As heterostructure, which contains a two-dimensional electrons gas 65 nm below the surface. Its electron density is  $n_s = 3 \times 10^{15} \text{ m}^{-2}$  and the elastic mean free path is  $l_e = 8 \mu\text{m}$  at  $T = 4.2 \text{ K}$ . A Hall bar is defined by wet etching and provided with Ohmic contacts (AuGe/Ni). The antidots as well as the square confining geometry pattern is produced by electron beam lithography, thus providing an inherently good alignment of the two structures. The square geometry around the finite antidot lattice has point contactlike openings at its corners serving as contacts to the system. The pattern is then transferred onto the sample by a carefully tuned wet etching step. The etch rate depends sensitively on the size of the respective features. In making the width of the bars that define the square confining geometry larger than the diameter of the antidots it is guaranteed that the finite lattice is decoupled from the outside 2DEG before the antidot potential is actually formed in the 2DEG. The inset of Fig. 2 shows an atomic force microscope image of the finite antidot lattice with a system size  $L = 2.4 \mu\text{m}$  and a period  $a = 240 \text{ nm}$ . Each antidot is well developed and the variation in size is remarkably small. The whole structure is covered by a gate metal, which allows one to tune the Fermi energy in the system. The sample is cooled in a dilution refrigerator down to bath temperatures of  $T = 30 \text{ mK}$ . Typical four-terminal measurements of the resistance  $R_{ij,kl}(B) = (U_k - U_l) / I_{i \rightarrow j}$

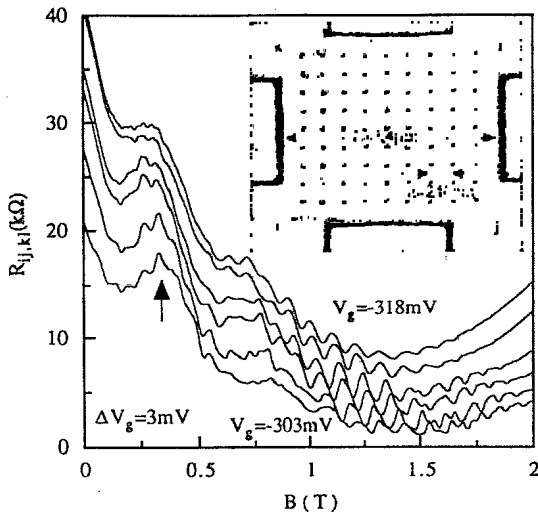


FIG. 2. Magnetoconductance traces of a finite antidot lattice at  $T = 30 \text{ mK}$  at very low carrier densities. The arrow indicates the classical commensurability maximum. The inset shows an image taken with an atomic force microscope of a wet etched surface of a GaAs/Al<sub>x</sub>Ga<sub>1-x</sub>As heterostructure with the characteristic dimensions as indicated. Ohmic contacts are made to the corners of the square indicated by  $i, j, k,$  and  $l$ .

are made by passing a current  $I$  through the contacts  $i$  and  $j$  and measuring the voltage drop across the other two contacts  $k$  and  $l$ .

In high magnetic fields the electrons in a homogeneous 2DEG travel along the boundary of the confining geometry in magnetic edge channels.<sup>9</sup> The suppression of backscattering leads to a quantized resistance in the Hall effect.<sup>10</sup> In our antidot samples edge states also develop along the circumference of the antidots. The electrons in these states are sensitive to the flux through the antidots if the phase coherence is maintained along the circumference. The edge states that form along the boundary of the square confining geometry are not sensitive to the flux through the antidots. However, if the Fermi energy  $E_F$  is lowered by a very negative gate voltage the constrictions between the walls and the antidots and between two neighboring antidots become very narrow. This leads to a coupling of the edge states that form at the edge of the confining geometry and the localized states around the circumference of the antidots.

Figure 2 presents the magnetoconductance  $R_{ij,kl}(B)$  for different negative gate voltages. At low magnetic fields  $B = 0.3 \text{ T}$  the resistance maximum corresponding to a classical orbit around a single antidot can be seen (see the vertical arrow). Superimposed on this classical commensurability maximum there are oscillations in the magnetoconductance that reveal an Aharonov-Bohm effect or, equivalently, a modified Shubnikov-de Haas effect related to the area enclosed by the classical cyclotron orbit that fits around a single antidot.<sup>6,7</sup> At higher magnetic fields a wide minimum occurs at about  $B \approx 1.5 \text{ T}$ , which is related to the minimum of the Shubnikov-de Haas oscillations at filling factor  $\nu = 2$ . The filling factor defined as  $\nu = hN_s / eB$  specifies the number of occupied Landau levels below the Fermi energy. A series of highly periodic AB oscillations with a period of  $\Delta B \approx 100 \text{ mT}$  arises in the magnetoconductance traces just in this  $\nu = 2$  minimum in the magnetic-field regime  $0.7 \text{ T} \leq B \leq 1.8 \text{ T}$ . The characteristic area leading to the AB oscillations is defined by the circumference of the antidots. The role of the classically pinned trajectories is now taken over by quantum-mechanical edge states also in the sense of commensurability effects. In single quantum dots such AB oscillations have been observed where the electrons are confined to edge states close to the perimeter of the dot.<sup>11,12</sup> Similar results were obtained by Kirczenow *et al.*,<sup>13</sup> who inserted a single antidot inside a narrow wire.

At high magnetic fields the energy of an edge channel is determined by its guiding center energy  $E_G = E_F - \hbar\omega_c(n + \frac{1}{2}) \pm g\mu_B B$ , where  $\omega_c$  is the cyclotron frequency,  $n$  is the Landau level index, and the last term accounts for spin splitting. The electrons follow the equipotential lines  $V(x, y) = E_G$  around the antidots. During one revolution they accumulate a phase  $\Delta\varphi = 2\pi\Phi / \Phi_0$ , where  $\Phi_0 = h/e$  is the elementary flux quantum. The resistance oscillations are periodic in  $B$ , corresponding to the addition of the one flux quantum through the enclosed area  $A(E_G)$ .

In order to get a quantitative understanding of the os-

cillations we Fourier transform the magnetoresistance as displayed in Fig. 3. If the window for the transformation is chosen around the minimum corresponding to  $\nu=2$ , pronounced maxima in the Fourier transforms are found. The maxima shift to higher frequencies  $f=(e/h)A(E_G)$  for more negative gate voltages. This is in agreement with the simple picture that with decreasing carrier density the antidots size increases. Consequently, the area given by the circumference of the antidots and the corresponding frequency of the AB oscillations increases. The inset of Fig. 3 shows the normalized frequency as a function of the applied gate voltage. The frequencies approach a value  $f=(e/h)A_0 \approx 11.5T^{-1}$ , which is determined by a circular area  $A_0=\pi(a/2)^2$  with the diameter equal to the lattice period. If the gate voltage is lowered further, the edge channels are reflected at the barriers between the antidots and the resistance diverges.

We have studied the behavior of the minimum in the magnetoresistance related to filling factor  $\nu=2$  in more detail for a different sample whose antidots are almost as large as the lattice period and are therefore larger than in sample 1 (Fig. 4). On this second sample the main features observed are very similar to what was described before. In particular, the gate voltage dependence of the AB period or, in other words, the area dependence follows the same trend. In this second sample the coupling between the edge channels can be achieved by applying moderate negative gate voltages. Therefore the mobility in the unpatterned regions remains comparatively high and the edge channels are spin resolved. The barrier height between the antidots can be adjusted by means of the gate voltage. At  $V_g = -200$  mV there are no oscillations present [lowest trace in Fig. 4(c)]. As the gate volt-

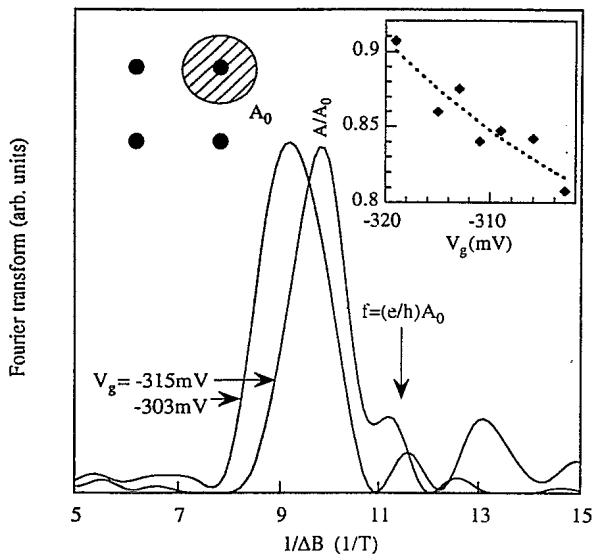


FIG. 3. Fourier transform calculated from the experimentally obtained magnetoresistance traces (Fig. 2). The right inset shows the dependence of the AB frequency on the applied gate voltage. The frequencies approach a value that is given by the circular area as indicated in the left inset.

age becomes more negative the coupling between edge states becomes apparent. The period of the oscillations in this case is only  $\Delta B \approx 50$  mT. At very strong depletion [Fig. 4(a)], we observe a doubling of the period of the oscillations. In between there is a transition regime where every second minimum of the oscillations is only weakly pronounced [Fig. 4(b)].

In order to explain the occurrence of the period doubling we discuss several possibilities. In general, a factor of 2 may arise by a transition from  $h/e$  to  $h/2e$  oscillations, the latter originating from the interference of time-reversed trajectories. However, it is not clear why the  $h/2e$  oscillations are only observed in a certain gate voltage regime. Since all scattering lengths (elastic and inelastic) decrease with increasing depletion, the  $h/2e$  oscillations should persist for negative gate voltages while the  $h/e$  effect could be averaged out more easily. This is

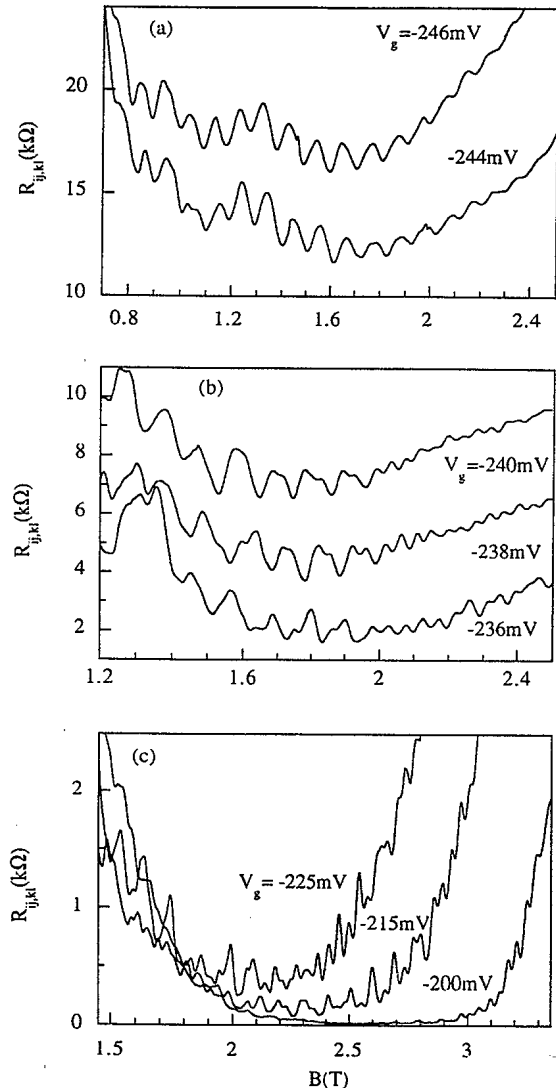


FIG. 4. Minimum of the magnetoresistance related to the filling factor  $\nu=2$ . At very strong depletion (c) every second minimum of the oscillations is suppressed, which leads to period doubling.

in contrast to our experimental observations. Another possibility is the contribution of edge channels that form in the region between four antidots. These may, in principle, provide an additional frequency. However, since they will enclose an area similar to the one defined by the circumference of the antidots, they can only accidentally provide a double frequency signal corresponding to an area twice as large.

On this basis we propose that the additional period is related to resonant processes between two spin-resolved edge channels. Quantum-mechanically bound states around the antidots exist if the enclosed flux is a multiple integer of the flux quantum  $A(E_G)B = \Phi_0(j + \frac{1}{2})$ , which corresponds to a phase change  $\Delta\varphi = 2\pi$ . This spatial quantization condition determines the energy  $E_{j,n}$  of the bound states around the antidots. Resonant transmission between bound states occurs if the Fermi energy  $E_F$  coincides with the energy of the bound states  $E_{j,n}$ . This situation is the basis of the following discussion. In Fig. 5 a schematic representation of the edge states at two different gate voltages is presented. For gate voltages that lead to low barriers between the antidots, both edge channels are fully transmitting. The bound states are spin resolved and are denoted  $\psi_{m,u}$  and  $\psi_{m,d}$ . Since spin is conserved in the resonant tunneling process, the current flows through states  $\psi_{m-1,d} \rightarrow \psi_{m,d} \rightarrow \psi_{m+1,d}$  and  $\psi_{m-1,u} \rightarrow \psi_{m,u} \rightarrow \psi_{m+1,u}$ . The subsequent minima in the resistance can be attributed to resonant tunneling of electrons with opposite spin. The observed phase between the two oscillations could be explained by a possible Coulomb interaction between the two edge states, as suggested by Sachrajda *et al.* for resonant reflection processes in a single quantum dot geometry.<sup>12</sup> Period doubling has also been observed in single antidot

geometries.<sup>13,14</sup> For higher potential barriers the edge channel with  $s=d$  is partly reflected while the  $s=u$  channel is fully transmitted. In this regime every second minimum is only weakly pronounced. Eventually the  $s=d$  channel is completely reflected and only the  $s=u$  channel contributes to the conductivity [Fig. 5(b)]. Resonant tunneling should in principle be independent of the thickness of the barrier. Our explanation relies on the assumption that the tunneling probabilities among spin-up and spin-down edge channels are comparable. For steep potential walls this could indeed be the case since the spatial separation between edge states could be small. However, for a more refined analysis one has to consider that in an antidot lattice each bound state interacts with the bound states of the four neighboring antidots and that both resonant tunneling and resonant reflection can occur.

At higher magnetic fields a series of  $B$ -periodic oscillations arises in the  $\nu=1$  minimum where only a single edge state is occupied. The oscillations in this regime have only a single period being related to the area of a single antidot. These observations support the idea that spin-related processes are responsible for the occurrence of the additional period. Further experiments may tell us which type of interpretation can lead to a physical picture.

Recently Lenssen *et al.*<sup>15</sup> reported on the observation of quantum interference in a two-dimensional lateral superlattice. They explained their observations by the phase-coherent coupling of localized classical orbits. Our experimental results as presented in this paper unambiguously demonstrate that AB oscillations occur in the edge state regime and that their frequency is related to the lattice period. In the sample as presented in Fig. 3, the Fermi wavelength is about  $\frac{1}{8}$  of the circumference of an antidot. In order to be able to observe Aharonov-Bohm oscillations the sample has to be homogeneous at least on that scale. For higher carrier densities the improved screening behavior will lead to an even more homogeneous sample. This fact, as well as the observation of pronounced fluctuations in the high-density regime,<sup>7</sup> implies that the phase coherence length in our system is at least of the order of the lattice dimension.

The fact that a four-terminal geometry is used in our experiment excludes the possibility that only a small fraction of the antidots or even antidots at the corners of the square predominantly give rise to the observed oscillations. In that sense the observation of Aharonov-Bohm oscillations in the edge state regime in a superlattice clearly constitutes a scenario different from experiments on single structures.<sup>12,14,16</sup>

In summary, we have reported on edge state transport through an antidot lattices with a finite number of periods ( $9 \times 9$ ). In the regime of small antidots and large carrier densities, commensurability oscillations are known to dominate the low-field magnetoresistance. In finite antidot lattices pronounced fluctuations are superimposed, reflecting the dominant role of chaotic trajectories in phase space.<sup>7</sup> In the present publication, however, where we concentrate on the quantum Hall regime, the survival of regular trajectories is thought to lead to

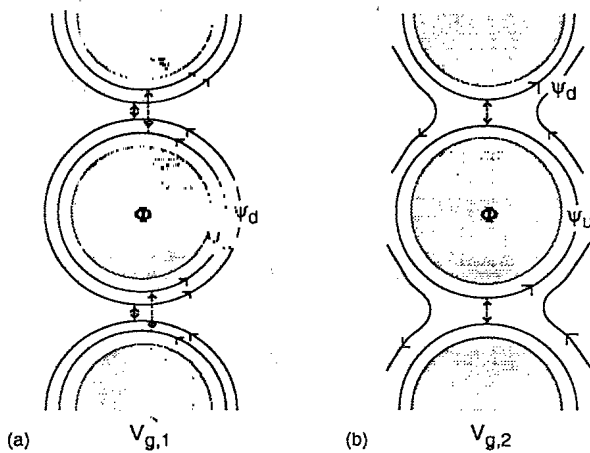


FIG. 5. Schematic representation of the edge channels for two different barrier heights between the antidots. The barrier height is adjusted by the gate voltage ( $V_{g,1} > V_{g,2}$ ). In (a) both spin-resolved edge channels are fully transmitted, which corresponds to the situation in Fig. 4(c). In (b) the second edge channel is reflected at the barriers between the antidots corresponding to the experimental trace in Fig. 4(a).

the transition to quantum-mechanical edge states. This is achieved with the application of a negative gate voltage, which lowers the Fermi energy such that the Fermi sea ends up being a shallow lake that just covers the minima of the potential. In this regime where transport is dominated by edge states, we observe AB-type oscillations superimposed on the Shubnikov-de Haas minimum corresponding to the filling factor  $\nu=2$ . The characteristic area for the AB oscillations is given by the circumferences of the antidots. By carefully adjusting the barrier

height between the antidots, the contribution of spin-resolved edge states can be observed.

It is a pleasure to thank T. Schlösser, M. Suhrke, and D. Wharam for most valuable discussions and M. Wendel for help with the atomic force microscope. We acknowledge financial support by the Deutsche Forschungsgemeinschaft (SFB 348) and the Volkswagen Stiftung (V.D.).

\*Present address: Department of Condensed Matter Physics, Braun Center for Submicron Research, Weizmann Institute of Science, Rehovot 76100, Israel.

†Present address: Laboratory for Solid State Physics, Swiss Federal Institute of Technology, ETH Hönggerberg, CH 8093 Zürich, Switzerland.

‡Permanent address: Institute of Solid State Physics, Chernogolovka, 142432 Moscow District, Russia.

<sup>1</sup>H. Fang, R. Zeller, and P. J. Stiles, *Appl. Phys. Lett.* **55**, 1433 (1989).

<sup>2</sup>K. Ensslin and P. M. Petroff, *Phys. Rev. B* **41**, 12 307 (1990).

<sup>3</sup>A. Lorke, J. P. Kotthaus, and K. Ploog, *Superlatt. Microstruct.* **9**, 103 (1991).

<sup>4</sup>D. Weiss, M. L. Roukes, A. Menschig, P. Grambow, K. v. Klitzing, and G. Weimann, *Phys. Rev. Lett.* **66**, 2790 (1991).

<sup>5</sup>R. Fleischmann, T. Geisel, and R. Ketzmerick, *Phys. Rev. Lett.* **68**, 1367 (1992).

<sup>6</sup>D. Weiss, K. Richter, A. Menschig, R. Bergmann, H. Schweitzer, K. v. Klitzing, and G. Weimann, *Phys. Rev. Lett.* **70**, 4118 (1993).

<sup>7</sup>R. Schuster, K. Ensslin, D. Wharam, S. Kühn, J. P. Kotthaus, G. Böhm, W. Klein, G. Tränkle, and G. Weimann, *Phys. Rev. B* **49**, 8510 (1994).

<sup>8</sup>A. Jacoby, U. Sivan, C. P. Umbach, and J. M. Jong, *Phys. Rev. Lett.* **66**, 1938 (1991).

<sup>9</sup>B. I. Halperin, *Phys. Rev. B* **25**, 2185 (1982).

<sup>10</sup>M. Büttiker, *Phys. Rev. B* **38**, 9375 (1988).

<sup>11</sup>B. J. van Wees, L. P. Kouwenhoven, C. J. P. M. Harmans, J. G. Williamson, C. E. Timmering, M. E. I. Broekhaart, C. T. Foxon, and J. J. Harris, *Phys. Rev. Lett.* **62**, 2523 (1989).

<sup>12</sup>A. S. Sachrajda, R. P. Taylor, C. Dharma-Wardana, P. Zawadzki, J. A. Adams, and P. T. Coleridge, *Phys. Rev. B* **47**, 6911 (1993).

<sup>13</sup>G. Kirczenow, A. S. Sachrajda, Y. Feng, R. P. Taylor, L. Henning, J. Wang, P. Zawadzki, and P. T. Coleridge, *Phys. Rev. Lett.* **72**, 2069 (1994).

<sup>14</sup>C. J. B. Ford, P. J. Simpson, I. Zailer, D. R. Mace, M. Yosefin, M. Pepper, D. A. Ritchie, J. E. F. Frost, M. P. Grimshaw, and G. A. C. Jones, *Phys. Rev. B* **49**, 17456 (1994).

<sup>15</sup>K.-M. H. Lenssen, M. E. J. Boonman, C. J. P. M. Kramans, and C. T. Foxon, *Phys. Rev. Lett.* **74**, 454 (1995).

<sup>16</sup>A. S. Sachrajda, Y. Feng, R. P. Taylor, G. Kirczenow, L. Henning, J. Wang, P. Zawadzki, and P. T. Coleridge, *Phys. Rev. B* **50**, 10856 (1994).